ISBN: 978-3-95450-262-2 ISSN: 2673-5350 doi: 10.18429/JACoW-IBIC2025-WEPMO23

PERFORMANCE RESULTS OF NOVEL PHOTOEMISSION MASK X-RAY BEAM POSITION MONITOR FOR 'WHITE' UNDULATOR RADIATION*

P. Ilinski†, MAX IV Laboratory, Lund, Sweden

Abstract

A prototype of a novel Photoemission Mask type X-ray Beam Position Monitor (PheM XBPM) for the 'white' undulator radiation which concept was proposed and has been built and tested. The prototype was designed and manufactured at MAX IV. Two PheM XBPMs were in-stalled at MAX IV 3 GeV storage ring at SoftiMAX and CoSAXS beamline frontends. Signal modelling, optimization and performance results of the PheM XBPM are discussed.

INTRODUCTION

Fixed mask is a component of the Storage ring beamline frontend, which function is to absorb unnecessary to beamline undulator radiation power. Fixed mask is a source of the photoelectrons, which can be used to determine undulator beam position. This kind of XBPM may not substitute the standard Blade type XBPMs, but due to a simple design and luck of heat load issues may be a worth to consider addition to beamline diagnostics.

DESIGN

The PheM XBPM [1] is utilising photoelectrons generated at upstream and downstream fixed masks under undulator radiation illumination. Fixed mask is a beamline frontend component, which function is to block and absorb most of undulator radiation, reducing transmitted to the beamline power.

The PheM XBPM upstream fixed mask has a rectangular exit aperture of 1.0 mrad x 1.0 mrad, Fig. 1, the downstream fixed mask has a rectangular exit aperture of 0.9 mrad x 0.9 mrad.

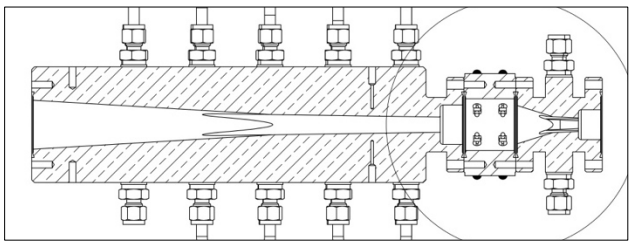

Figure 1: PheM XBPM design: (from left to right) upstream fixed mask, readout, downstream mask.

PheM XBPM has upstream and downstream sets of four electrodes. Each electrode has a SMA feedthrough with push-on connector. Two sets of electrodes were chosen for prototype version to explore various electrostatical and signal readout configurations. Electrodes are positioned at 45 degrees to vertical axis, and 2 mm away from the corners of upstream exit aperture, so they are not exposed to direct undulator radiation (Fig. 2 left).

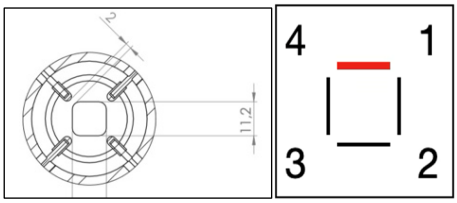

Figure 2: PheM XBPM electrodes locations (right), exit aperture surfaces with electrodes numbering (left).

SIGNAL MODELING

Undulator spectral calculations were performed using SRW program [2]. Photoelectron signal is the product of undulator spectrum and copper total electron yield (TEY). Undulator radiation flux spectral density for CoSAXS 2-m-long, 19.3-mm-period planar undulator at K=1.25 (gap 7.42 mm) is show at Fig. 3 along with copper TYE and resulting signal on-axis and at 1 mrad. As can be seen, at 1 mrad beam direction, photoelectron signal is dominated by 200 eV energy photons.

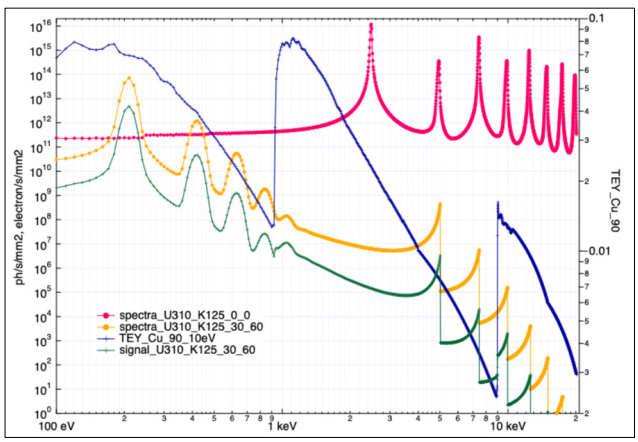

Figure 3: CoSAXS undulator radiation flux spectral density, K=1.25: on-axis (pink), 1 mrad (yellow). Copper TEY (blue). Signal spectral density at 1 mrad (green).

Once the incident photon spectre is known, we can estimate the resulting spectra of primary and secondary electrons. Electron spectra calculations were performed for incident photon energy of 200 eV and different configurations with Sessa program [3]. Total yield electron (TYE) for copper is shown at Fig. 4. Electron signal modelling allows to estimate energy distribution of the produced photo-electrons. As can be seen at Fig. 4, low energies secondary electrons are dominating, making an extended continuum.

* Research conducted at MAX IV is supported by the Swedish Research council (contract 2018-07152), the Swedish Governmental Agency for Innovation Systems (contract 2018-04969), and Formas (contract 2019-02496)
†petr.ilinski@maxiv.lu.se

ISBN: 978-3-95450-262-2 ISSN: 2673-5350 doi: 10.18429/JACoW-IBIC2025-WEPMO23

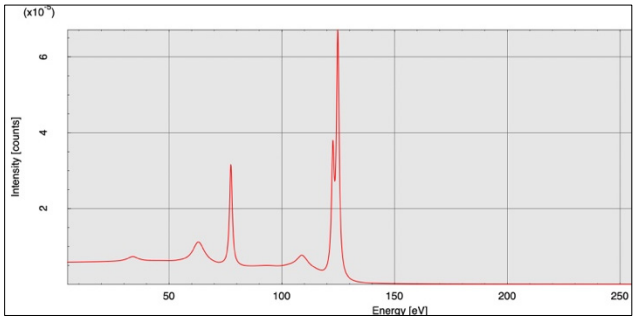

Figure 4: Copper TYE spectra for 200 eV incident photons.

The CST Studio [4] was used for the electrostatic simulations and electrons trajectories transport. Four surfaces of the fixed mask exit aperture were treated as a separate photoemission electrodes (Fig. 2, right). The electrons trajectories from upper fixed mask surface to the PheM XBPM electrodes biased at 100V are show at Fig. 5.

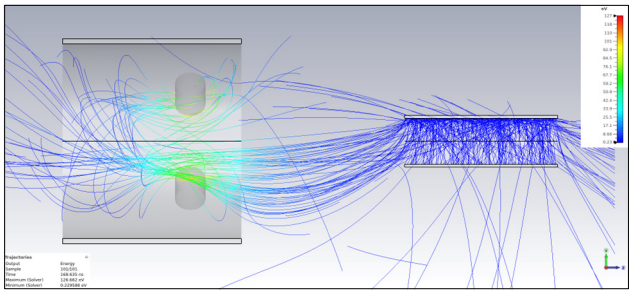
Figure 5: 1 eV electrons trajectories, emitted from the upper surface of exit aperture, electrodes bias is 100 V.

As can be seen at Fig. 5, at 100 V bias most of the 1 eV electrons trajectories are directed to the bottom electrodes. By changing the bias voltage applied to the electrodes, the electrons trajectories and electrons energy distribution reached the electrodes can be controlled. By adjusting the electrodes bias one can try to maximize the difference between signals of upper and bottom electrodes, increasing PheM XBPM position sensitivity.

The number of electrons reaching the upper electrode #4 and bottom electrode #3 for a range of electrodes bias voltages of - 200 V to + 400 V and for electrons initial energies in the range of 1 eV to 1000 eV are shown in Figs 6 and 7. Difference for +10 V bias has a better signal ratio for the low energy electrons. While at - 10 V bias, the difference is achieved for higher energy electrons at much lower signal.

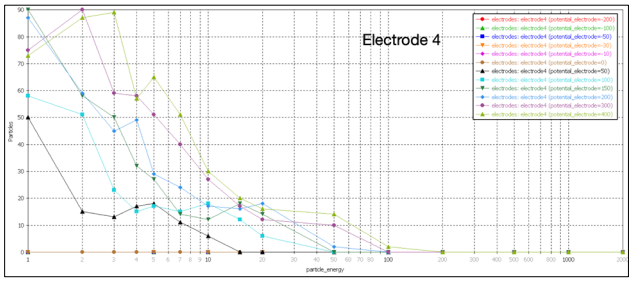

Figure 6: Number of electrons reached electrode #4 for various electrodes bias voltages and initial electron energies.

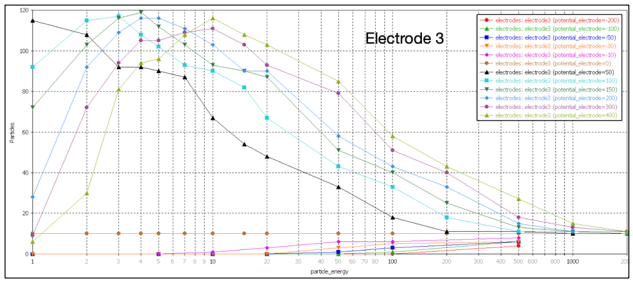

Figure 7: Number of electrons reached electrode #3 for various electrodes Bias voltages and initial electron energies.

BEAM POSITION MEASUREMENTS

The sum of four electrodes currents versus bias voltage measurement with CoSAXS planar undulator K=1.25 (gap = 7.42 mm) are shown at Fig. 8. Total signal is about - 7 μA at zero bias voltage, it is reaching -32 μA at +200 V bias voltage. By appling negative bias voltage low energy electrons start to be repelled from the electrodes. Total signal is reduced to 0.3 μA at negative bias of -45 V.

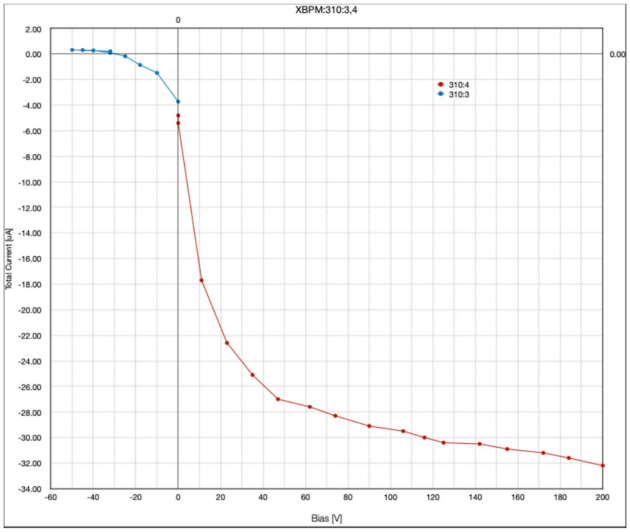

Figure 8: PheM XBPM total signal (sum of four electrodes currents) vs Bias voltage.

CoSAXS frontend has two photoemission blade XBPM1 and XBPM2 installed at 12 m and 16 m from the undulator centre. PheM XBPM is installed downstream from the Fixed Mask at 11.5 m. PheM XBPM, has two sets of four readout electrodes, XBPM3 is upstream, XBPM4 is downstream. Vertical and horizontal XBPMs measurements at bias voltages applied to the XBPM3 of +13V and XBPM4 of -28V and for angular e-beam Local Bump 2 μrad step are presented at Figs. 9 and 10. Vertical position at the PheM XBPM3,4 depends on the storage ring current. In case of MAX IV the injection occurs every ten minutes, topping up from 396 mA to 400 mA.

Vertical and horizontal positions at PheM XBPM at bias voltages of -1 V for both readouts and for various e-beam Local Bumps are shown at Figs. 11 and 12. The Local Bump steps are: y' = 2 μrad, y = +/- 20 μm, x'=2 μrad, x = 20 μm. For this bias settings, vertical position of XBPM3,4 much more sensitive to the Local Bump vertical

ISBN: 978-3-95450-262-2 ISSN: 2673-5350 doi: 10.18429/JACoW-IBIC2025-WEPMO23

offset. XBPM3 is following offset and angle, while XBPM4 does not.

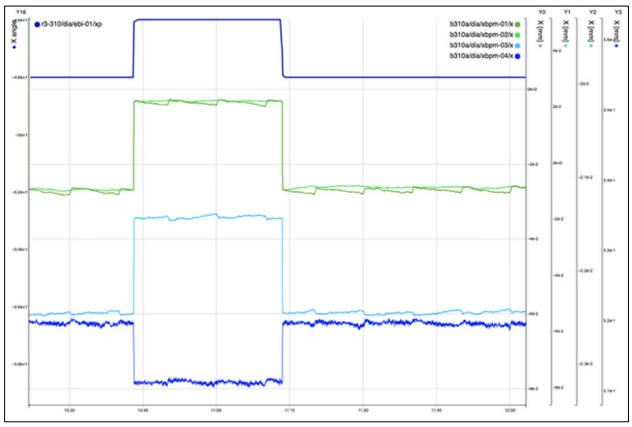

Figure 9: Horizontal position CoSAXS XBPM1,2 and PheM XBPM3,4. E-beam 2-µrad-step angle, bias voltages: XBPM3 +13V, XBPM4 -28 V.

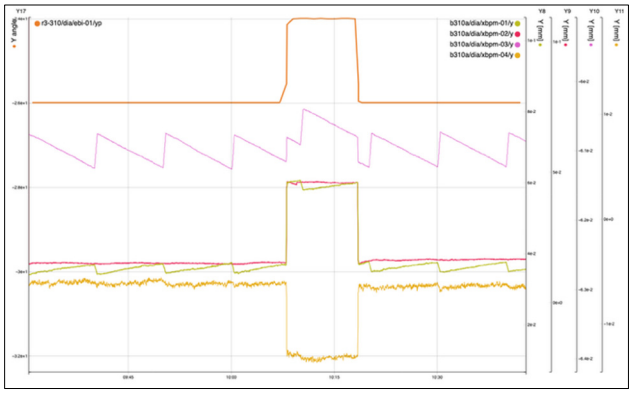

Figure 10: Vertical position CoSAXS XBPM1,2, PheM XBPM3,4. E-beam 2-µrad-step angle, bias voltages: XBPM3 +13V, XBPM4 -28 V.

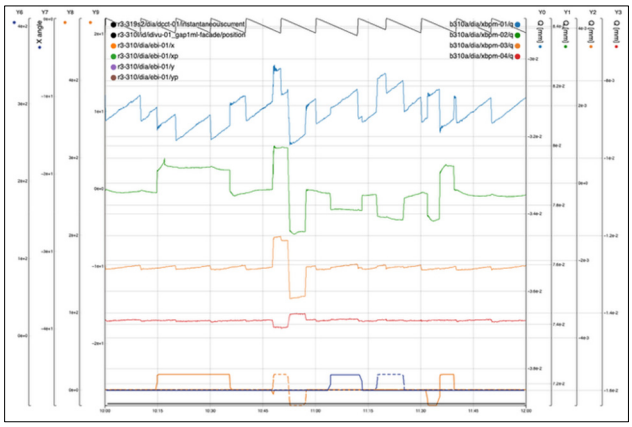

Figure 11: Vertical XBPMs positions for Local Bump: y' = 2 µrad, y = +/- 20 µm, x'=2 µrad, x = 20 µm, bias -1 V.

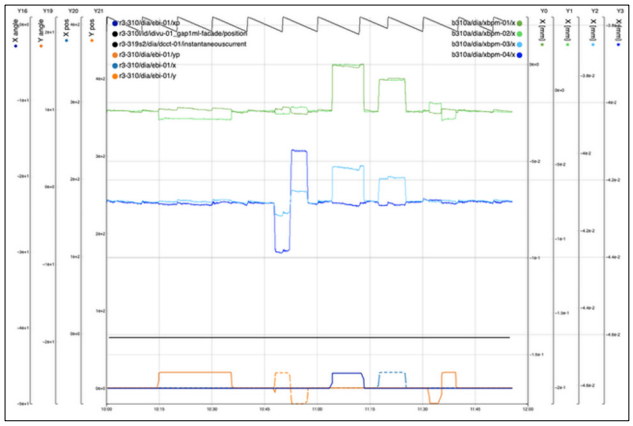

Figure 12: Horizontal XBPMs positions for Local Bump: y' = 2 µrad, y = +/- 20 µm, x'=2 µrad, x = 20 µm, bias -1 V.

A strong coupling between vertical Local Bump and horizontal position of the XBPM4 can be observed, Fig. 12.

CONCLUSION

Since PheM XBPM has low cost, do not intercept the undulator beam, it can be considered as a supplemental diagnostics tool. Relation of the PheM XBPM positions to the e-beam direction may not be straightforward and depends on the electrodes bias potentials. The optimal design, operation parameters and reaction to various types of e-beam Local Bumps need further investigation and interpretation.

REFERENCES

[1] P. Ilinski, "Novel Photoemission Type X-Ray Beam Position Monitor for the 'White' Undulator Radiation", in *Proc. IBIC'22*, Kraków, Poland, Sep. 2022, pp. 159-162. doi:10.18429/JACoW-IBIC2022-MOP44

[2] O. Chubar and P. Elleaume, "Accurate and Efficient Computation of Synchrotron Radiation in the Near Field Region", in *Proc. EPAC'98*, Stockholm, Sweden, Jun. 1998, paper THP01G, pp. 1177-1179.

[3] W. Werner, W. Smekal, and C. Powell, *Simulation of Electron Spectra for Surface Analysis (SESSA) Version 2.2.2 User's Guide*, National Institute of Standards and Technology, Gaithersburg, MD, USA, 2024. doi:10.6028/NIST.NSRDS.100-2024

[4] CST Studio, https://www.3ds.com/products/simulia/cst-studio-suite